TITLE:
Theory of Phase Transitions in Solid Methanes. The James-Keenan Model with an Octahedral Crystalline Field(Dissertation_全文)

AUTHOR(S):
Kataoka, Yosuke

CITATION:
Kataoka, Yosuke. Theory of Phase Transitions in Solid Methanes. The James-Keenan Model with an Octahedral Crystalline Field. 京都大学, 1970, 理学博士

ISSUE DATE:
1970-03-23

URL:
https://doi.org/10.14989/doctor.r1581

RIGHT:

京都大学学術情報リポジトリ
KURENAI 紅
Kyoto University Research Information Repository

学位論文

片岡洋右

主論文

Theory of Phase Transitions in Solid Methanes. VI

The James-Keenan Model with an Octahedral Crystalline Field*)

Yosuke KATAOKA

Department of Chemistry, Faculty of Science,

Kyoto University, Kyoto, Japan

---

*) A preliminary report of this work was read at the International Conference on Statistical Mechanics, held at Kyoto, September 1968.

Abstract

The James-Keenan model which is extended by inclusion of a crystalline field of octahedral symmetry is studied with the purpose of elucidating the mechanism of phase transitions and the nature of molecular rotation in the solid methane. All the calculations are made in the subspace $J \leq 4$, J being the rotational quantum number. Four types of solid phase are examined, three of which are assumed to have the same sublattice structures and the same symmetry relations as the disordered phase and the low and high temperature ordered phases of James and Keenan's classical theory, and the remainder has a layer structure. First, nuclear spin species A and T are treated separately. Then normal mixture of these nuclear spin species is examined with a further assumption that these nuclear spin species are randomly distributed in the lattice. A simplest possible form of octahedral field is assumed. The strength of the field is taken from the analysis made by Cabana, Savitsky and Hornig of the infrared absorption spectra by methane molecules dispersed in the matrix of Kr and Xe crystals. It is shown that thermodynamic properties of the extended James-Keenan model are similar to those of the original one and normal mixture exhibits the observed double transitions in solid methane when the magnitude of the effective

octopole moment is chosen such that the observed upper transition temperature is reproduced. Nuclear spin species A is shown to be more stable than species T, which is in conformity with Wong, Noble, Bloom and Alexander's and Runolfsson, Mango and Borghini's experiments on the mean square value of the proton angular momentum at low temperatures. The effects of variation of both the magnitude of the effective octopole moment and the strength of the crystalline field are also discussed.

1. Introduction

Methane has recently been attracting much attention as an object of study on the molecular dynamics in the condensed phase at low temperatures. From infrared spectra of solid CH_4 and CD_4 and dilute solutions in one another at temperatures ranging from 5 to 40°K, Savitsky and Hornig[1] concluded that free rotation as the disordering mechanism seems to be ruled out for all the transitions[2)-9)] in the solid state. They estimated from the observed line width the barrier as high as several hundred cm^{-1}. Glasel[10] observed near-infrared absorption spectra of solid methane in the regions of $\nu_1+\nu_4$ and $\nu_3+\nu_4$ over a temperature range from 6 to 33°K. He did not find any evidence of molecular rotation so that he was led to an interpretation relying upon an order-disorder transition mechanism. Ewing[11] studied infrared absorption of the ν_3-fundamental of CH_4, CD_4, and solutions of CD_4 in CH_4 in the liquid and solid states from 105 down to 28°K. The observed broad liquid-state absorption is consistent with the assumption that molecules make slightly hindered rotation in the liquid state. Furthermore, the band width decreases gradually with decreasing temperature and undergoes no discernable discontinuous change on passing through the freezing point, which suggests that the rotatory motion persists even in the solid state. Ewing estimated the height of barrier as 63 cm^{-1} in the liquid state. From the fact that the narrow

band observed at 28°K ($\Delta\nu$=15 cm^{-1}) lacks librational structure it was suggested that the rotational barrier does increase as the temperature is lowered.[11] Raman spectra of liquid and crystalline methane were observed by Crawford, Welsh and Harrold[12] and by Anderson and Savoie.[13] Crawford et al. attributed the complicated shape of the ν_2 and ν_3 vibration bands in the liquid state to conservation of the quantum nature of rotation of the molecules.[11] Spectra of the higher-temperature solid phase (at 77°K) by Anderson and Savoie were very similar to those in the liquid state. This again suggests that molecular rotation persists in the crystal at temperatures near the melting point.[13] Anderson and Savoie's observation was also supported by neutron inelastic scattering experiments[14),15)] in liquid state. Gordon[16] disclosed a close relation between the infrared and Raman spectra by looking at the time correlation functions associated with molecular rotation. The main conclusion of his arguments is that both spectra allow us to derive a consistent view of hindered rotations.

Dorner and Stiller[17] derived frequency distributions of solid CH_4 at 2.7, 18 and 84°K from the energy distributions of scattered neutrons and found no evidence of free rotation. Harker and Brugger[18] performed slow neutron scattering experiments at temperatures 5, 9.1, 18 and 22.1°K. Comparison of the 22°K data with Griffing's "discrete rotation gas model"[19] almost eliminates the possibility of free rotational

motion at this temperature.[18] The width of the elastic scattering peak was analyzed by Sköld.[20] He suggested that the broadening of the elastic peak is due to frequent stepwise reorientation of molecules and estimated the average time between successive rotational jumps as about 10^{-12} sec at T=22.1°K. On the other hand, Thiele, Whitney and Chase[21] measured the velocity and attenuation of ultrasonic waves in the solid state and pointed out that their data above the λ-point are consistent with a single relaxation process the characteristic time τ of which increases sharply with decreasing temperature. They obtained $\tau \sim 5\times10^{-8}$ sec at T_λ, a value that compared with Tomita's value[22] $\tau_c \sim 10^{-7}$ sec (at the same temperature) which was obtained by analysis of T_1 of the proton magnetic resonance observed by Thomas, Alpert and Torrey.[23] However, Sandhu, Lees and Bloom[24] recently reported that Thomas, Alpert and Torrey's T_1 values are about 1000 times as short as those in pure CH_4. DeWitt and Bloom[25] measured the proton and deuteron spin-lattice relaxation time T_1 in CH_4, CD_4, CHD_3, CH_3D, and CH_4-CD_4 mixtures and CH_4-krypton mixtures as a function of temperature between 1.2 and 60°K. Their analysis of the data revealed that the strong temperature dependence of T_1 is associated with molecular reorientation. They obtained $\tau_c \sim 8\times10^{-11}$ sec at 18°K. From what was mentioned so far, it is now obvious that there are significant barriers to rotation of methane molecules even in the disordered phase (highest temperature phase).

As for the theoretical studies of the phase transitions, James and Keenan[4] predicted classically the structure of the three solid phases in solid CD_4 together with the double transition in conformity with experiment[2] under the assumption of electrostatic octopole-octopole interaction between neighboring molecules whose carbon atoms form a rigid FCC lattice. Yamamoto et al. have developed a quantum statistical mechanical study of the model in a series of papers, I,[5] II,[6] III,[7] and V[8], with the same title as the present one, for the purpose of verifying whether the model is capable of reproducing the observed remarkable quantum effects in solid CH_4 and CH_3D.[2] The upper transition temperatures in solid CH_3D and CHD_3 and solid solutions of CH_4 and CD_4 were also calculated in IV.[9] From the results of these studies it has been proved that the James-Keenan model is quite hopeful as a working model for understanding the nature of the phase transitions in the whole family of the isotropic solid methanes. Owing to the very nature of the molecular field approximation employed, the molecules are never affected by a hindering potential in the disordered phase.

In order to get rid of this defect, we will proceed one step further in the present article by including a crystalline field to the original James-Keenan model. This extention takes into account a part of the effect of the dispersion force and the valence force[26] that was neglected in James

and Keenan's assumption[4] of electrostatic octopole-octopole interaction. As an approximation, we use a crystalline field which a methane molecule feels in a xenon or krypton crystal, since a CH_4 molecule fits almost exactly into a substitutional hole in those crystals. Cabana, Savitsky and Hornig[27] reported the infrared spectra of CH_4 and CD_4, present as substitutional impurities in crystals of argon, krypton and xenon, at temperatures ranging from 5 to 40°K. The theory of the hindered rotational levels of a sperical top in an octahedral field was worked out in considerable detail by King and Hornig.[28] Based on this theory, Cabana, Savitsky and Hornig[27] estimated the barrier to rotation about a fourfold crystal axis as 50-60 cm^{-1} for CH_4 in xenon. This result is used in the present calculation. The strength of the crystalline field is assumed to be constant against temperature. The quantum statistical mechanical properties of this extended James-Keenan model are studied by the molecular field approximation. All the calculations are made in the subspace $J \leqq 4$, J being the rotational quantum number. Four types of solid phase are examined, three of which are assumed to have the same sublattice structures and

the same symmetry relations as the disordered phase and the low and high temperature ordered phases of James and Keenan's classical thoery, and the remainder has a layer structure. First, nuclear spin species A and T are treated separately. Then normal mixture of these nuclear spin species is examined with a further assumption that these nuclear spin species are randomly distributed in the lattice.

It will be shown that thermodynamic properties of the extended James-Keenan model are similar to those of the original one and normal mixture exhibits the observed double transitions in solid methane, provided that the magnitude of the effective octopole moment is chosen such that the observed upper transition temperature is reproduced. Nuclear spin species A is more stable than species T and this result is compatible with Wong, Noble, Bloom and Alexander's[29] and Runolfsson, Mango and Borghini's[30] experiments on the mean square value of the proton angular momentum at low temperatures. The other cases where the magnitude of the effective octopole moment and the strength of the crystalline field are changed will be also discussed.

2. Formulations

The Crystalline Field

We assume the simplest form for the octahedral crystalline field, which is written in terms of the rotational function $\mathcal{D}^{(4)}_{M,M'}(\omega)$ as follows,[28]*)

$$V(\omega) = \beta_4 B\left[\frac{7}{4}\mathcal{D}^{(4)}_{0,0}(\omega) + \frac{\sqrt{70}}{8}\left\{\mathcal{D}^{(4)}_{0,4}(\omega) + \mathcal{D}^{(4)}_{0,-4}(\omega) + \mathcal{D}^{(4)}_{4,0}(\omega) + \mathcal{D}^{(4)}_{-4,0}(\omega)\right\}\right.$$
$$\left. + \frac{5}{8}\left\{\mathcal{D}^{(4)}_{4,4}(\omega) + \mathcal{D}^{(4)}_{-4,-4}(\omega) + \mathcal{D}^{(4)}_{4,-4}(\omega) + \mathcal{D}^{(4)}_{-4,4}(\omega)\right\}\right], \tag{2.1}$$

where ω is the Euler angles and B is the rotational constant of a free methane molecule and β_4 is a dimensionless parameter. This is normalized such that

$$\int d\omega\, V(\omega)^2 = (\beta_4 B)^2 \cdot 8\pi^2. \tag{2.2}$$

---

*) Frayer and Ewing[31] used another expression of the crystalline field in the analysis of the infrared spectra of methane in an argon matrix.

The strength of the crystalline field is estimated as $\beta_4=-4$ from the analysis made by Cabana et al.[11] of their infrared absorption spectra by methane molecules dispersed in the matrix of Kr and Xe crystals.

The crystalline field (2.1) can be expressed in a more explicit form

$$V(\{\alpha\beta\gamma\}) = \beta_4 B\Big[\frac{7}{4}\Big(1-5\sin^2\beta+\frac{35}{8}\sin^4\beta\Big) + \frac{35}{32}\sin^4\beta(\cos 4\alpha+\cos 4\gamma) + \frac{5}{4}\Big(1-\sin^2\beta+\frac{1}{8}\sin^4\beta\Big)\cos 4\alpha\cos 4\gamma - \frac{5}{4}\cos\beta\Big(1-\frac{1}{2}\sin^2\beta\Big)\sin 4\alpha\sin 4\gamma\Big]. \tag{2.3}$$

The coordinate system fixed in the lattice and the standard orientation of molecule are shown in Figs. 2 and 1 in II,[6] respectively. From this expression one sees that the x, y and z axes are the four-fold rotation axes,

$$V(\{\alpha,0,0\}) = \beta_4 B\Big(\frac{7}{4}+\frac{5}{4}\cos 4\alpha\Big). \tag{2.4}$$

For minus values of β_4, the crystalline field has the minimum

value $3\beta_4 B$ for $\omega=\{0, 0, 0\}$ and $\{\pi/2, 0, 0\}$ and for the equivalent orientations and the maximum value $(-13/9)\beta_4 B$ for $\omega=\{\pi/4, \beta, \pi/4\}$ with $\sin^2\beta=8/9$ and for the equivalent orientations. These orientations of the potential minima where the hydrogens are oriented toward the cube corners seem probable since in these orientations all protons of the methane molecule under consideration are simultaneously at the maximum distance from the center of mass of the three neighboring methane molecules. For this reason it seems reasonable that the sign of β_4 has been chosen minus.

The Molecular Field Approximation

A quantum statistical mechanical formulation of the original James-Keenan model has been developed in great details in II.[6] Since addition of the crystalline field brings no new difficulties, only a brief outline of the formulation may be given here. First the assumptions and approximations employed are summarized below.

(a) The electrostatic octopole-octopole interaction is assumed between nearest neighboring pairs of methane molecules in an FCC lattice*) (the James-Keenan model[4]). In addition

---

*) Recent x-ray analysis revealed that the carbon atoms form an FCC lattice in the temperature range 4.2 to 75°K.[32]

to that, each molecule is assumed to feel the crystalline field $V(\omega)$ of octahedral symmetry (2.1).

(b) The molecular motion is studied in the subspace spanned by the rotational wave functions of a free molecule with $J \leq 4$, J being the rotational angular momentum quantum number.

(c) The molecular field approximation is employed.

(d) Four types of solid phase are examined, three of which are assumed to have the same sublattice structures and the same symmetry relations as the disordered phase and the low and high temperature ordered phases of James and Keenan's classical theory.[4] The remaining phase has a layer structure as shown in Fig. 1, where the signs of the molecular fields in each of two sublattices are opposite. This is called the 2-sublattice antiferrorotational phase.

(e) No interspecies conversion occurs.*)

(f) When we say "normal mixture" of nuclear spin species A and T it is meant that the abundance ratio of A and T is conventionally fixed at 5:11. These nuclear spin species are assumed to be randomly distributed in the lattice.

The octopole-octopole interaction is written down, as was proved in I[5] of the present series,

---

*) "Equilibrium mixture" is left for future study, where interspecies conversion occurs quickly enough to attain the true equilibrium.

$$U(1,2) = U_0 \sum_{M,m} C(336; M-m, m) Y^*_{6,M}(\theta,\phi) \times \left\{ \mathcal{D}^{(3)}_{-2,M-m}(\omega_1) - \mathcal{D}^{(3)}_{2,M-m}(\omega_1) \right\} \times \left\{ \mathcal{D}^{(3)}_{-2,m}(\omega_2) - \mathcal{D}^{(3)}_{2,m}(\omega_2) \right\}, \tag{2.5}$$

$$U_0 = I_3^2 r^{-7} (3 \cdot 7 \cdot 11 \cdot 4\pi / 13)^{\frac{1}{2}}, \tag{2.6}$$

where ω_1 and ω_2 stand for the Euler angles of the orientations of respective molecules, r, θ and ϕ the polar coordinates of the relative position of the two molecules, and I_3 the octopole moment. Hereafter, $\xi = I_3^2 r^{-7}$ is called a coupling parameter.

Under the assumption (a), we put the Hamiltonian in the form

$$\mathcal{H} = \sum_i K(i) + \sum_{(i,j)} U_{ij}(i,j) + \sum_i V(i), \tag{2.7}$$

where $\sum_{(i,j)}$ means the summation over nearest neighbor pairs. Now we introduce the so-called molecular field

$$\tilde{U}_i(i) = \sum_j \mathrm{tr}^{(j)} U_{ij}(i,j) \rho_j(j), \tag{2.8}$$

where ρ is the one-molecule density matrix

$$\rho = \frac{1}{Z} \exp -\beta (K + \tilde{U} + V) . \qquad (2.9)$$

The consistency equations are written in terms of the molecular fields,

$$\tilde{U}_i(i) = \sum_j \mathrm{tr}^{(j)} U_{ij}(i,j) \frac{1}{Z_j} \exp -\beta [K(j) + \tilde{U}_j(j) + V(j)] . \qquad (2.10)$$

From (2.5) it is clear that

$$\tilde{U}_i(i) = \sum_\nu \alpha_{i\nu} \{ \mathcal{D}^{(3)}_{-2,\nu}(\omega_i) - \mathcal{D}^{(3)}_{2,\nu}(\omega_i) \} , \qquad (2.11)$$

where the coefficients $\alpha_{i\nu}$ are to be determined as a function of temperature.

The existence of the disordered phase can be seen from the following discussions on symmetry. The crystalline field $V(\omega)$ is a basis of the irreducible representation A_1 of the octahedral rotation group, while $\mathcal{D}^{(3)}_{-2,\nu}(\omega) - \mathcal{D}^{(3)}_{2,\nu}(\omega)$ are the bases of the irreducible representation A_2 of the same group.[33] For this reason, if we put $\tilde{U}_j(j)=0$ on the right-hand side of

Eq.(2.10), the value of the right-hand side vanishes, so that we have the disordered phase as a solution of (2.10) at any temperature.

The 2-sublattice Antiferrorotational Phase

As the 2-sublattice antiferrorotational phase*) is a new one in the present series of investigations, its formulation may be given in this subsection.

For the 2-sublattice antiferrorotational phase, the consistency equations (2.10) are written in terms of molecular field $\tilde{U}^{I}$ and $\tilde{U}^{II}$,

$$\tilde{U}^{I} = \sum_{2} tr^{(2)} U(1/I, 2/I) \frac{1}{Z^{I}} \exp -\beta(K+\hat{U}^{I}+V)$$
$$+\sum_{2} tr^{(2)} U(1/I, 2/II) \frac{1}{Z^{II}} \exp -\beta(K+\hat{U}^{II}+V), \qquad (2.12)$$

*) By a classical calculation,[34] it can be shown that in the limit of $\beta_4=-\infty$ an octopolar array in the FCC lattice is most stable in the layer structure shown in Fig.1. In this limit, molecules on site I have the orientation $\omega=\{0, 0, 0\}$ and molecules on site II have the orientation $\omega=\{\pi/2, 0, 0\}$.

$$\tilde{U}^{II} = \sum_{2} tr^{(2)} U(1/II, 2/I) \frac{1}{Z^I} \exp -\beta(K+\hat{U}^I+V)$$
$$+\sum_{2} tr^{(2)} U(1/II, 2/II) \frac{1}{Z^{II}} \exp -\beta(K+\tilde{U}^{II}+V). \quad (2.13)$$

The assumption (d) says $\tilde{U}^{II}=-\tilde{U}^{I}$. Observing that functions $\mathcal{D}^{(3)}_{-2,\nu}(\omega)$ $-\mathcal{D}^{(3)}_{2,\nu}(\omega)$ change their sign by rotation$\{\pi/2, 0, 0\}$ about the molecular C_Z axis, one sees that this assumption means the molecular field $\tilde{U}^{II}$ referred to this rotated system is the same as $\tilde{U}^{I}$ in the original system. From this relation, Eqs. (2.12) and (2.13) are reduced to a consistency equation in terms of $\tilde{U}^{I}$

$$\tilde{U}^{I} = \sum_{2} tr^{(2)}\{U(1/I, 2/I) - U(1/I, 2/II)\}$$
$$\times \frac{1}{Z^I} \exp -\beta(K+\hat{U}^I+V). \quad (2.14)$$

This equation is the same as that of the ferrorotational phase if $\mathcal{Y}^*_F$ in II (4.1) and II (4.2)[6] is replaced by $\mathcal{Y}^*_{2\text{-AF}}$.

The definition of $\mathcal{Y}^{*}_{2\text{-AF}}$ is as follows,

$$\mathcal{Y}^{*}_{2\text{-AF},M} = \sum_{\sigma/\mathrm{I}} Y^{*}_{6,M}(\theta_\sigma, \phi_\sigma) - \sum_{\sigma/\mathrm{II}} Y^{*}_{6,M}(\theta_\sigma, \phi_\sigma), \tag{2.15}$$

and their numerical values are given below,

$$\mathcal{Y}^{*}_{2\text{-AF},M} = \begin{cases} -1.783906 & \text{if } M=\pm 4 \\ -0.0635692 & \text{if } M=0 \\ 0 & \text{otherwise.} \end{cases} \tag{2.16}$$

If we put $\beta_4=0$, the linearized consistency equation of (2.14) determines the branching temperature vs coupling parameter relation (cf. II (4.35)[6]),

$$G(\beta) = -1/1.30495 , \tag{2.17}$$

which corresponds to an even phase in the sense of II:[6]

$$\begin{aligned} \alpha_{-2} &= \alpha_2 \\ \alpha_\nu &= 0 \quad \text{if } \nu \neq \pm 2 . \end{aligned} \tag{2.18}$$

The molecular field in this phase can be expressed with $u_1(\omega)$, which is one of the tetrahedral rotation functions of James and Keenan.[4] Comparing this with II (4.35),[6] and remembering

the definition of the $G(\beta)$, one can conclude that the values of the coupling parameter for the ferrorotational and 2-sublattice antiferrorotational phases which correspond to a particular value of the branching temperature obey the relation

$$\xi_{2\text{-}AF} / \xi_F = 2.25 . \qquad (2.19)$$

This shows that the 2-sublattice antiferrorotational phase is less stable than the ferrorotational phase if $\beta_4=0$.

The nonlinear consistency equation (2.14) was numerically solved by an iteration method with the restriction of $J \leqq 4$. All the results will be explained in the next section together with those for the other phases.

3. Results of the numerical calculations and discussions

As was already mentioned in Sec. 2, the value of β_4 is fixed at -4 throughout the present calculations, unless otherwise stated.

Nuclear Spin Species A

Figure 2 shows branching temperature vs ξ curves for the three ordered phases. From this Figure one sees that the values of the coupling parameter for the ferrorotational and 8-sublattice antiferrorotational phases which correspond to a particular value of branching temperature obey the relation $\xi_F/\xi_{8\text{-}AF}=1.017$. In Fig. 3, the free energy vs ξ curves for the three ordered phases at 2°K are shown. Figs. 4 and 5 give two examples of free energy vs temperature curves. There appears a single transition at 23.7°K, below which the 8-sublattice antiferrorotational phase survives in Fig. 4. One sees double transitions in Fig. 5, where the high temperature ordered phase is the 8-sublattice antiferrorotational phase and the low temperature phase is the ferrorotational phase. The phase diagram is shown in Fig. 6, where the abscissa is the coupling parameter ξ. The region in which the 2-sublattice antiferrorotational phase is most stable is very narrow. Comparing these results with those shown in II,[6] one sees that the crystalline field assumed does not appreciably affect the thermodynamic properties of nuclear spin species A.

Nuclear Spin Species T

In Fig. 7, the branching temperature vs ξ curves are shown. Figure 8 shows the free energy vs ξ curves at 2°K. Figure 9 gives free energy vs temperature curves for ξ=3.40°K. One sees double transitions, the upper one being at 21.3°K and the lower one at 16°K. The high and low temperature ordered phases are identified with the 8-sublattice antiferrorotational and ferrorotational phases, respectively. This figure is compared with Fig. 14 in II.[6] The 2-sublattice antiferrorotational phase does not appear at all temperatures at this value of ξ.

Repeating numerical calculations at other values of ξ, we obtain the phase diagram as shown in Fig. 10. From this figure one sees that double transitions such as shown in Fig. 9 occur for the values of ξ>3.28°K. In the region 3.16°K<ξ<3.28°K, one sees new double transitions, the high and low temperature ordered phases are identified with the 8-sublattice antiferrorotational and 2-sublattice antiferrorotational phases, respectively. For smaller values of ξ, i.e., 1.79°K<ξ<3.16°K, we have a single transition, where the low temperature phase is the 2-sublattice antiferrorotational phase. This can be understood as follows: As the value of β_4 is fixed as -4, the effect of the crystalline field becomes larger for smaller values of ξ.

Normal Mixture

Figure 11 shows branching temperature vs ξ curves for the three ordered phases of normal mixture. As the observed upper transition temperature is 20.4°K,[2] the high temperature ordered phase is identified to the 8-sublattice antiferrorotational phase. The numerical value, 3.40°K, which was temporarily assigned to ξ in the case of species T, yields the upper transition at 20.5°K this time. We will adopt this value here again because it will make easier the comparison of the results of normal mixture with those of pure species T. Remembering that the upper transition temperature is 19.5°K for the same value of ξ if $\beta_4=0$,[7] one see that the addition of the crystalline field makes only a little difference in this respect. The free energy vs temperature curves are plotted in Fig. 12 for normal mixture. One sees double transitions, the upper one being at 20.5°K, as was stated above, and the lower one at 13.5°K. The low temperature ordered phase is identified with the ferrorotational phase. The 2-sublattice antiferrorotational phase cannot appear in this case. The lower transition is a first order transition and its latent heat can be estimated from the difference of the internal energy at the transition temperature, which is equal to 0.86 cal/mole. Perhaps a better comparison of theory and experiment is that in terms of the total heat of transition in a finite temperature range about the transition. The present theory gives 3.64 cal/mole for the temperature

range from 12°K to 14°K. This may be compared with the observed value 4.4 cal/mole which is associated with the broad anomaly in the specific heat at around 8°K.[2] As regards the upper transition, Clusius[35] has reported a heat of transition of 18.1 cal/mole for the temperature range from 17°K to 21°K, while the present theory gives 13.6 cal/mole for the same temperature range. With this comparison, the extended James-Keenan model applied to normal mixture with ξ=3.40°K and β_4= -4 seems compatible with the observed double transitions in solid methane. This is one of the most important results of the present study. Figure 13 shows the free energy vs ξ curves at 2°K. There is a critical value ξ_c=3.35°K of coupling parameter at this particular temperature. That is to say, if $\xi<\xi_c$, the ferrorotational phase is less stable than the 2-sublattice antiferrorotational phase and vice versa. The phase diagram of normal mixture is shown in Fig. 14.

Comparison of Free Energies and of Rotational Energy Levels

Free energies at 0°K, ξ=3.40°K are listed up in Table 1. From this Table one sees that pure species A is most stable, which is in conformity with the observation by Wong, Noble, Bloom and Alexander[29] and by Runolfsson, Mango and Borghini[30] on the mean square value of the proton spin angular momentum at low temperatures. It is now obvious that we will eventually have to study equilibrium mixture, where interspecies conversion

occurs quickly enough to attain the true equilibrium. We will not go into this subject here, leaving it for future study. Only discussions based on the calculations on normal mixture may be added here. A few lowest rotational energy levels at 0°K, ξ=3.40°K are shown in Table 2. From the comparison of the rotational levels of species A and T in normal mixture, one at once sees that species T will convert into A if the conversion is allowed at all.*)

From Table 2 one sees some differences in the degeneracies of the rotational levels in the ferrorotational and 2-sublattice antiferrorotational phases in normal mixture (cf. III Figs. 3 and 4).[7] This evidently is due to the differences of the symmetries of the effective potentials, which may be important in the analysis of spectroscopic data.

---

*) Owing to the very nature of the molecular field approximation employed, the internal energy is not the mere average of the eigenvalue of the one-molecule effective Hamiltonian (i.e. the rotational energy levels) but the average minus a half of the interaction energy. For this reason, we cannot compare the lowest rotational levels of pure A and those of T to see which is more stable at low temperatures. The statement on normal mixture is rather reliable because the molecular fields are determined consistently in the single homogeneous phase.

Comments on the Crystalline Field

We have examined the effects of the crystalline field by varying its strength. The free energy vs coupling parameter curves have been obtained of the three ordered phases and the disordered phase at 2°K for various values of β_4. The results are summarized in Figs. 15 and 16 for species A and normal mixture, respectively, where the sections at 2°K of phase diagrams are shown (cf. Figs. 6 and 14). In the case of normal mixture the point marked by ξ=3.40°K and β_4=-4 is in the ferrorotational phase, near the boundary of the 2-sublattice antiferrorotational phase. As was stated in the preceding subsection, the extended James-Keenan model applied to normal mixture with ξ=3.40°K and β_4=-4 seems compatible with the observed double transitions in solid methane in respect of the thermodynamical properties. However, in view of the situation just mentioned, we are not in a position to definitely say which the lowest temperature phase should be assigned to the ferrorotational or 2-sublattice antiferrorotational phase. Thus the present study shows that the effects of the crystalline field to the James-Keenan model are so important that further studies are needed with the more realistic crystalline field which may be derived from the analysis of the spectroscopic data, especially, of the disordered phase*)

---

*) See, for example, Solt's examination of the effects of the rotational hindrance on neutron scattering for solid methane at 86°K.[35)]

and from the molecular-theoretical calculations on intermolecular forces.

Acknowledgements

The present work has been started with the suggestion by Professor T. Yamamoto. The author would like to thank him for his continual guidance and encouragement.

The author is also indebted to the members of Quantum Chemistry Laboratory, especially to Dr. K. Okada, Mr. H. Yasuda Mr. K. Nishiyama and Mr. S. Hirokawa for valuable suggestions and discussions. He also thanks to Mr. H. Yasuda for his numerical computational aid. He acknowledges Kyoto University Computation Center, Kyoto University Data Processing Center and "Computer Centre, University of Tokyo" for services and computer time made available for this study.

References

1) G.B.Savitsky and D.F.Hornig, J. Chem. Phys. 36 (1962), 2634.

2) For calorimetric studies see J.H.Colwell, E.K.Gill and J.A.Morrison, J. Chem. Phys. 39 (1963), 635; 42 (1965), 3144. The first includes a very nice survey of the literatures on solid methane up to 1963.

3) L.Pauling, Phys. Rev. 36 (1930), 430.

4) H.M.James and T.A.Keenan, J. Chem. Phys. 31 (1959), 12.

5) T. Yamamoto, J. Chem. Phys. 48 (1968), 3193.

6) T.Yamamoto and Y.Kataoka, J. Chem. Phys. 48 (1968), 3199; Phys. Rev. Lett. 20 (1968), 1.

7) Y.Kataoka and T.Yamamoto, Prog. Theor. Phys. Suppl. Extra Number (1968), 436.

8) K.Nishiyama, Y.Kataoka and T.Yamamoto, to be published.

9) H.Yasuda, T.Yamamoto and Y.Kataoka, Prog. Theor. Phys. 41 (1969), 859.

10) J.A.Glasel, J. Chem. Phys. 34 (1961), 1649.

11) G.E.Ewing, J. Chem. Phys. 40 (1964), 179.

12) M.F.Crawford, H.L.Welsh and J.H.Harrold, Can. J. Phys. 30 (1952), 81.

13) A.Anderson and R.Savoie, J. Chem. Phys. 43 (1965), 3468.

14) Y.D.Harker and R.M.Brugger, J.Chem. Phys. 42 (1965), 275.

15) S.Hautecler and H.Stiller, Z. Physik 166 (1962), 393. But see also: B.A.Dasannacharya and G.Venkataraman, Phys. Rev. 156 (1967), 196.

16) R.G.Gordon, J. Chem. Phys. 43 (1965), 1307.

17) B.Dorner and H.Stiller, Inelastic Scattering of Neutrons, (International Atomic Energy Agency, Vienna, 1965), Vol.2, p. 291. See also: H.Stiller and S.Hautecler, Inelastic Scattering of Neutrons in Solid and Liquid, (International Atomic Energy Agency, Vienna, 1963), Vol.2, p. 281.

18) Y.D.Harker and R.M.Brugger, J. Chem. Phys. 46 (1967), 2201.

19) G.W.Griffing, Inelastic Scattering of Neutrons in Solid and Liquid, (International Atomic Energy Agency, Vienna, 1963), Vol.1, p. 435.

20) K.Sköld, J. Chem. Phys. 49 (1968), 2443.

21) A.A.Thiele, W.M.Whitney and C.E.Chase, Low-Temperature Physics, LT9, J.G.Daunt et al., Eds. (Plenum Press, Inc., New York, 1965), Pt. B, p. 1122.

22) K.Tomita, Phys. Rev. 89 (1953), 429.

23) J.T.Thomas, N.L.Alpert and H.C.Torrey, J. Chem. Phys. 18 (1950), 1151.

24) H.S.Sandhu, J.Lees and M.Bloom, Can. J. Chem. 38 (1960), 443.

25) G.A.de Wit and M.Bloom, Can. J. Phys. 47 (1969), 1195.

26) For intermolecular forces of methane molecules, see, for example: S.Kimel, A.Ron, D.F.Hornig, J. Chem. Phys. 40 (1964), 3351.

27) A.Cabana, G.B.Savitsky and D.F.Hornig, J. Chem. Phys. 39 (1963), 2942.

28) H.F.King and D.F.Hornig, J. Chem. Phys. 44 (1966), 4520.

29) K.P.Wong, J.D.Noble, M.Bloom and S.Alexander, J.Magnetic Res. 1 (1969), 55.

30) Ö.Runolfsson, S.Mango and M.Borghini, private communication.

31) F.H.Frayer and G.E.Ewing, J. Chem. Phys. 48 (1968), 781.

32) S.C.Greer and L.Mayer, Z. Angew. Phys. 27 (1969), 198.

33) See, for example: S.L.Altmann and A.P.Cracknell, Rev. Mod. Phys. 37 (1965), 19.

34) Y.Kataoka and T.Yamamoto, to be published.

35) K.Clusius, Z. Phys. Chem. B3 (1929), 41.

36) G.Solt, Physica 37 (1967), 253.

Figure Captions

Fig. 1. The sublattice structure of the layer structure, open circle represents the sublattice I and solid circle the sublattice II.

Fig. 2. The branching temperature T_b vs coupling parameter ξ curves of species A. $\beta_4=-4$. The dashed, solid and dashed-dotted curves correspond to the 8-sublattice antiferrorotational (II), ferrorotational (III) and 2-sublattice antiferrorotational phases (IV), respectively.

Fig. 3. Free energy of species A as a function of ξ at 2°K. $\beta_4=-4$. The arrow indicates the critical value $\xi_c=3.82$°K.

Fig. 4. Free energy vs temperature plots of species A in the case of $\xi<\xi_c$. $\xi=3.68$°K. $\beta_4=-4$. F_{dis} denotes free energy of the disordered phase (I). The symbol of lines is the same as that in Fig. 2. The disordered phase (I) and the 8-sublattice antiferrorotational phase (II) can appear but not the ferrorotational phase (III), nor the 2-sublattice antiferrorotational phase (IV).

Fig. 5. Free energy vs temperature plots of species A in the case of $\xi>\xi_c$. $\xi=4.0$°K. $\beta_4=-4$. The symbol of lines is the same as that in Fig. 2. Both ferrorotational (III) and 8-sublattice antiferrorotational phases (II) exist and thus double transitions are seen, but the 2-sublattice

antiferrorotational phase (IV) cannot appear.

Fig. 6. Phase diagram of species A, $J \leq 4$. $\beta_4=-4$. Symbols I, II, III and IV denote the disordered, 8-sublattice antiferrorotational, ferrorotational and 2-sublattice antiferrorotational phases, respectively.

Fig. 7. The branching temperature T_b vs coupling parameter ξ curves of species T. $\beta_4=-4$. The symbol of lines is the same as that in Fig. 2.

Fig. 8. Free energy of species T as a function of ξ at 2°K. $\beta_4=-4$. The symbol of lines is the same as that in Fig. 2. The arrow indicates the critical value $\xi_c=3.28$°K.

Fig. 9. Free energy vs temperature plots of species T. $\xi=3.40$°K. $\beta_4=-4$. F_{dis} denotes free energy of the disordered phase (I). The symbol of lines is the same as that in Fig. 2.

Fig. 10. Phase diagram of species T, $J \leq 4$. $\beta_4=-4$. Symbols I, II, III and IV denote the disordered, 8-sublattice antiferrorotational, ferrorotational and 2-sublattice antiferrorotational phases, respectively.

Fig. 11. The branching temperature T_b vs coupling parameter ξ curves of normal mixture. $\beta_4=-4$. The symbol of lines is the same as that in Fig. 2.

Fig. 12. Free energy vs temperature plots of normal mixture. ξ=3.40°K, β_4=-4. F_{dis} denotes free energy of the disordered phase (I). The symbol of lines is the same as that in Fig. 2.

Fig. 13. Free energy of normal mixture as a function of ξ at 2°K. β_4=-4. The symbol of lines is the same as that in Fig. 2. The arrow indicates the critical value ξ_c=3.35°K.

Fig. 14. Phase diagram of normal mixture, $J \leqq 4$. β_4=-4. Symbols I, II, III and IV denote the disordered, 8-sublattice antiferrorotational, ferrorotational and 2-sublattice antiferrorotational phases, respectively.

Fig. 15. The section of phase diagram of species A at 2°K, where the intensity of the crystalline field, β_4 and the coupling parameter of octopole-octopole interaction, ξ are variables. Symbols I, II, III and IV are the same as those in Fig. 14.

Fig. 16. The section of phase diagram of normal mixture at 2°K, where β_4 and ξ are variables. Symbols I, II, III and IV are the same as those in Fig. 14.

Table 1. Free Energy of Solid Methane (R°K)
at 0°K, ξ = 3.40°K, β_4 = -4.

	Pure Species A	Pure Species T	Normal Mixture
Disordered Phase	-6.666	9.092	4.168
Ferrorotational Phase	-	5.506	2.071
2-sublattice Antiferro-rotational Phase	-6.674	5.860	2.218

Table 2. A Few Lowest Rotational Energy Levels (°K)

at 0°K, ξ = 3.40°K, β_4 = -4.

(The level J=0 is chosen as the zero point.)

Normal Mixture		Normal Mixture	
Species T	Species A	Species T	Species A
2-sublattice Antiferrorotational Phase		Ferrorotational Phase	
82.64 (3)*)	109.62 (3)	25.28 (1)	81.95 (2)
52.80 (2)	80.58 (3)	24.20 (2)	72.22 (1)
36.90 (3)	56.15 (1)	-12.81 (1)	41.29 (1)
-2.80 (3)	-14.68 (1)	-13.54 (2)	-24.56 (1)

*) Numbers in the parentheses indicate degeneracies.

Table 2. A Few Lowest Rotational Energy Levels (°K)

at 0°K, ξ = 3.40°K, β_4 = -4.

(The level J=0 is chosen as the zero point.)

(continued)

Pure Species T		Pure Species A	
Ferro-rotational Phase	Disordered Phase	2-sublattice Antiferro-rotational Phase	Disordered Phase
24.30 (1)	84.19 (3)	109.93 (3)	109.94 (3)
23.20 (2)	53.92 (2)	84.17 (3)	84.29 (3)
-16.46 (1)	30.42 (3)	52.36 (1)	52.22 (1)
-17.32 (2)	9.09 (3)	-6.93 (1)	-6.67 (1)

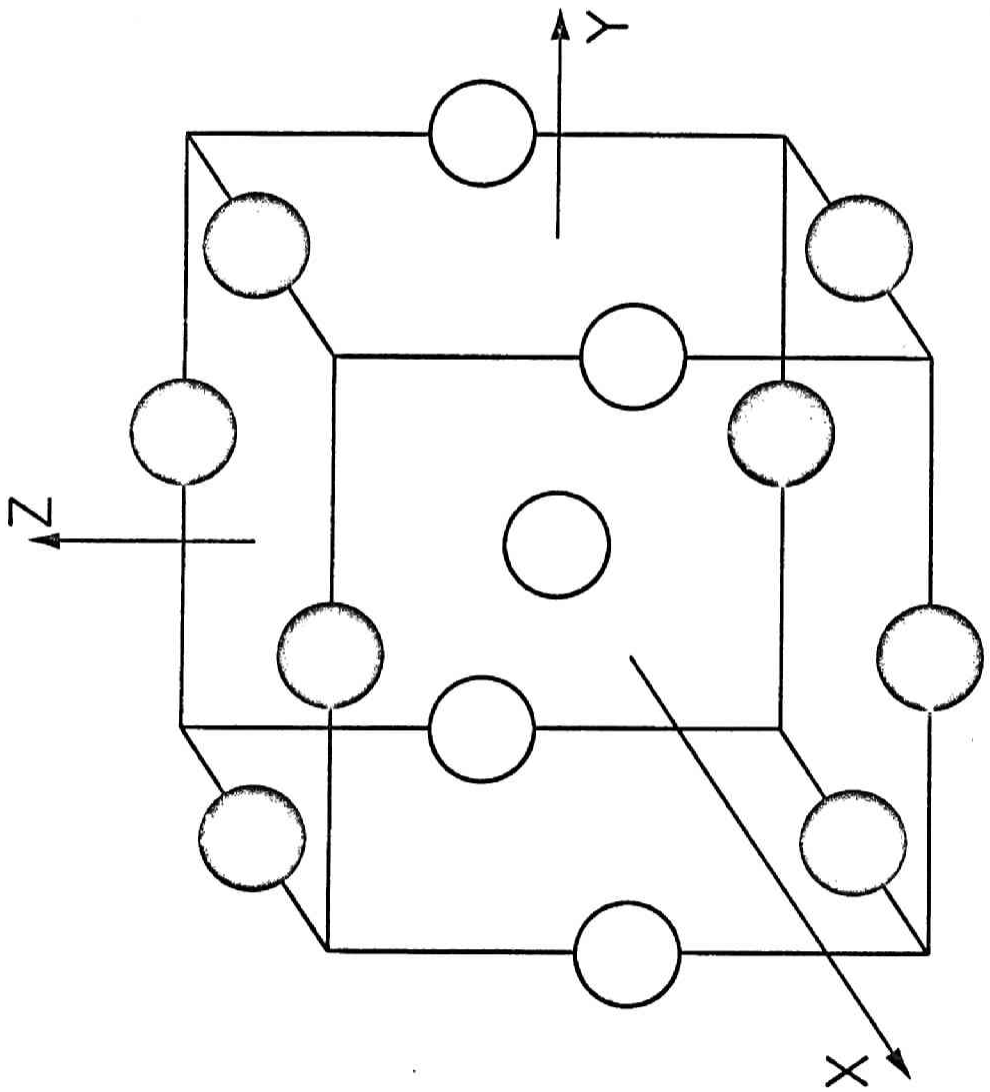

Fig. 1.

Fig. 2.

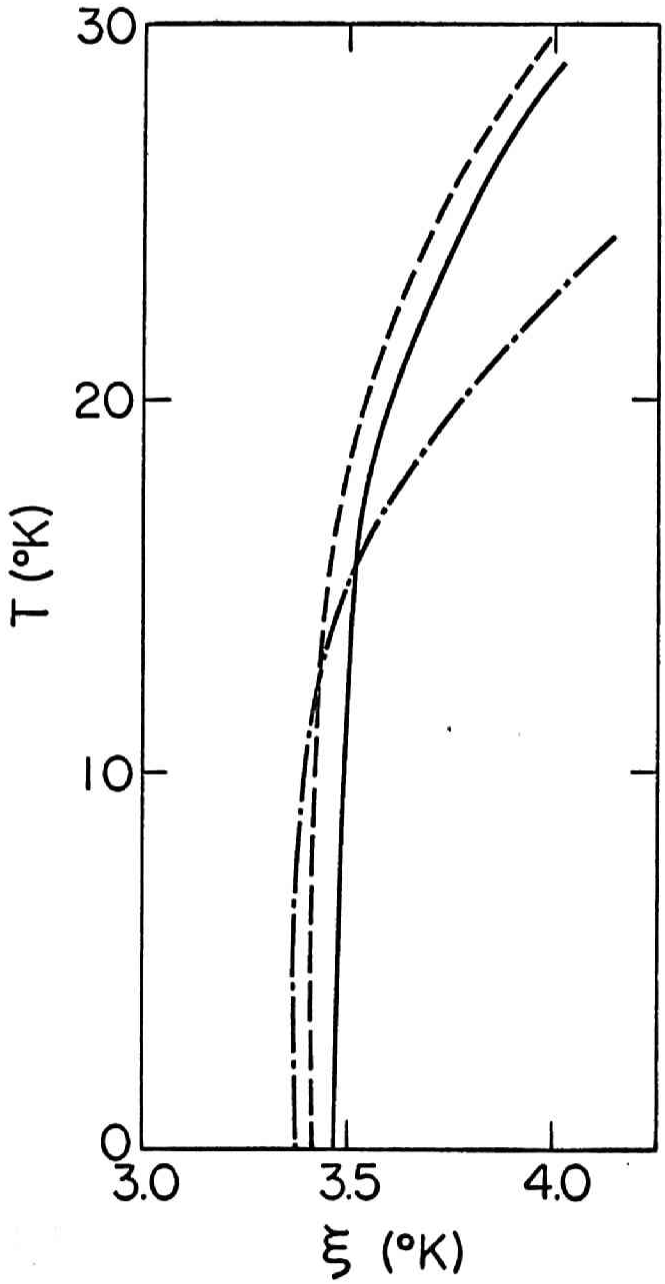

Fig. 3.

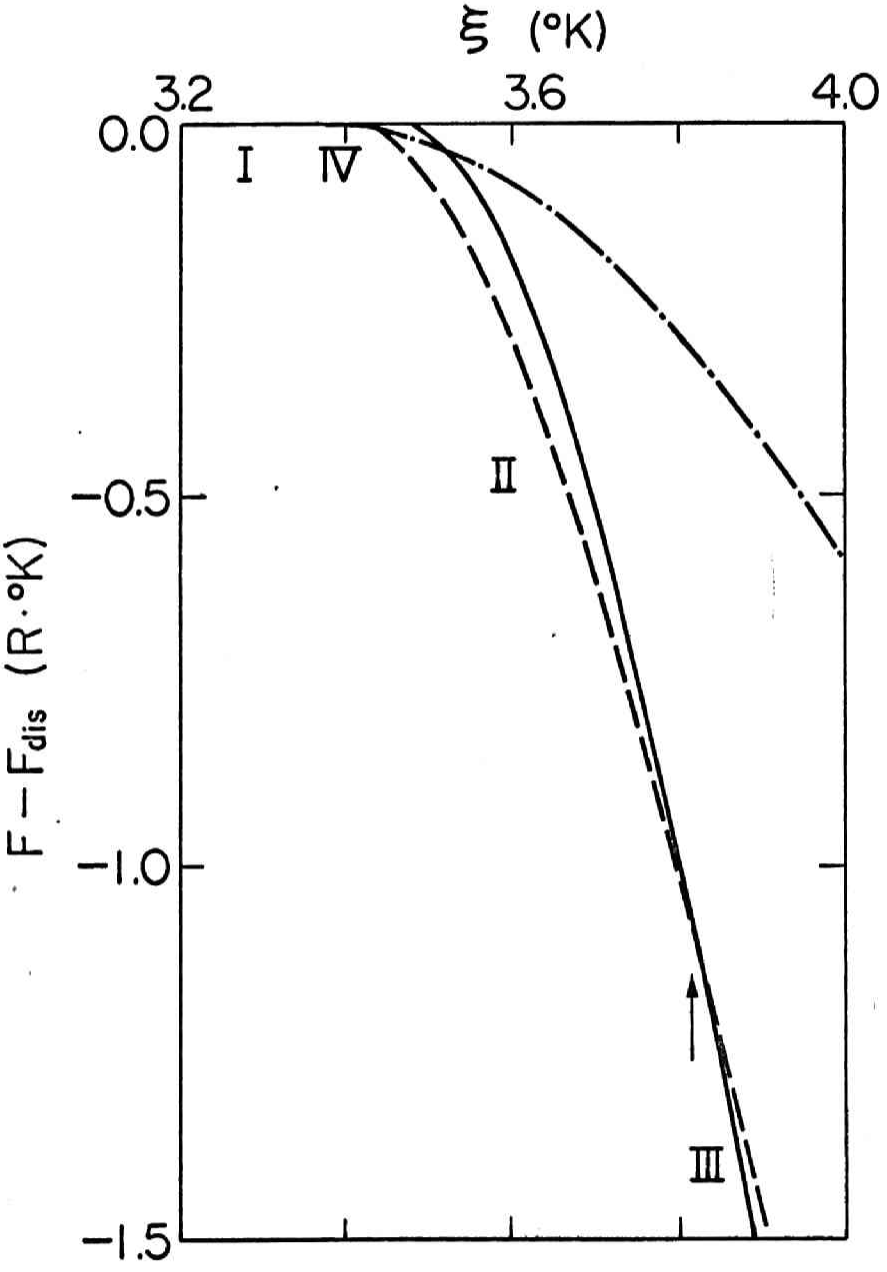

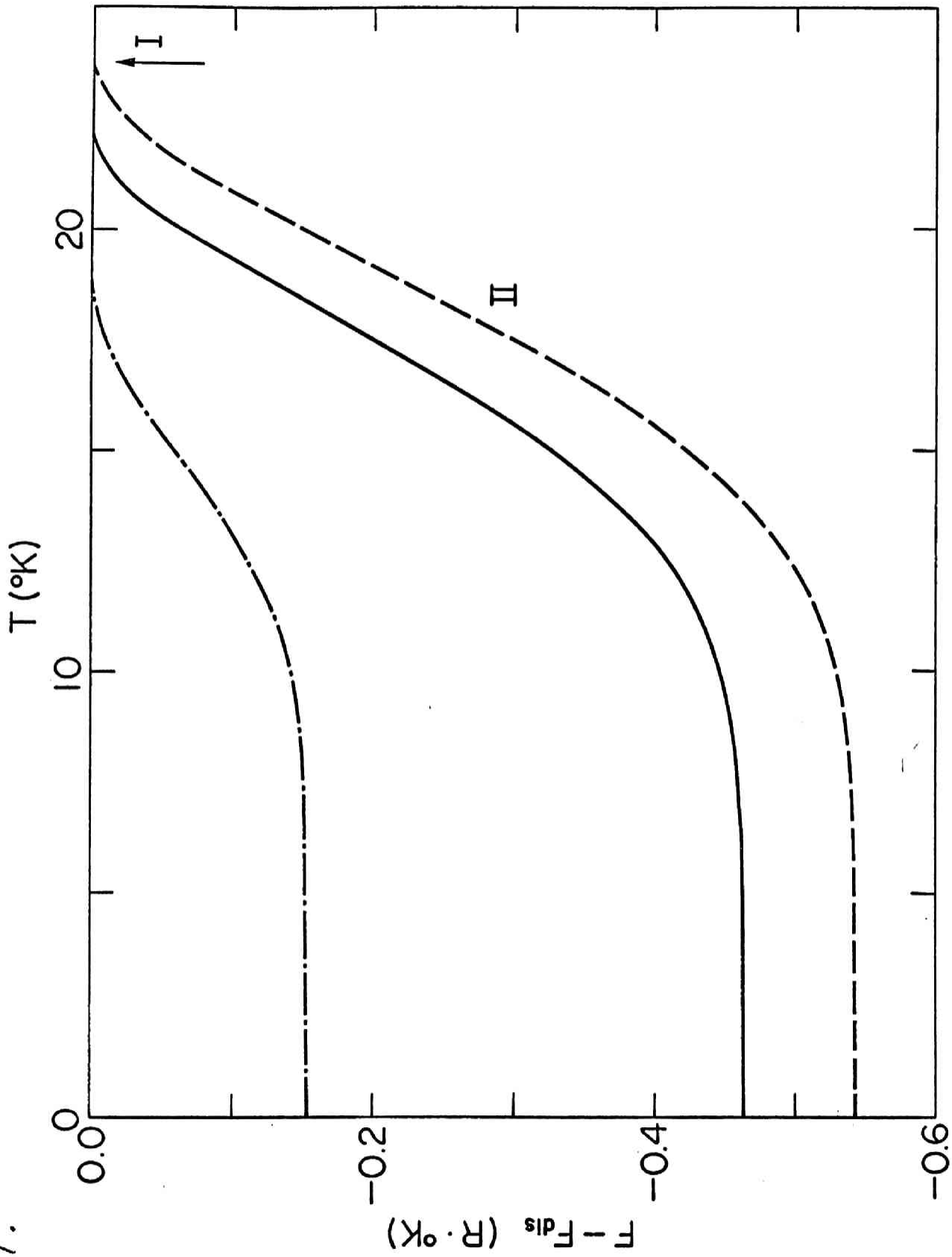

Fig. 4.

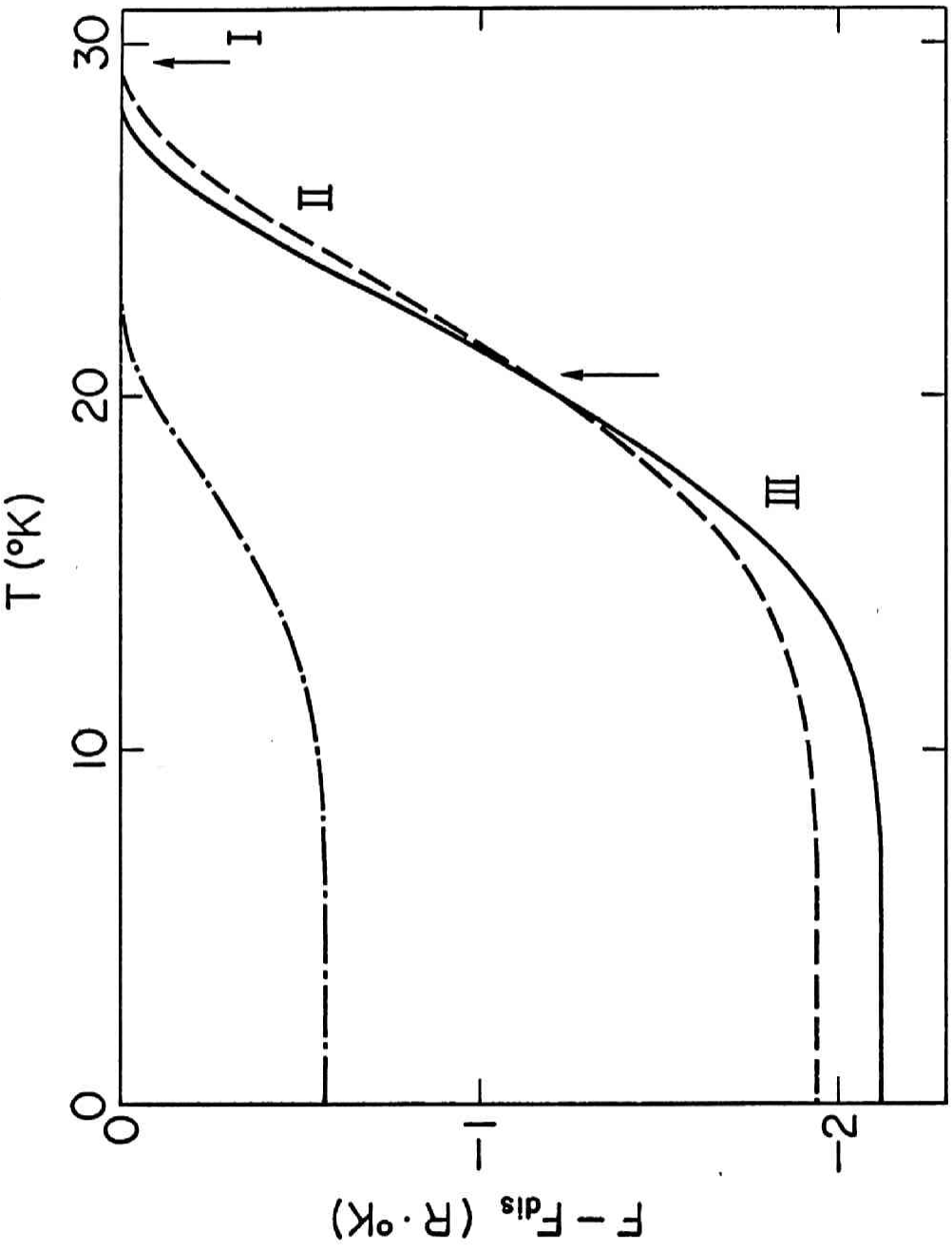

Fig. 5.

Fig. 6.

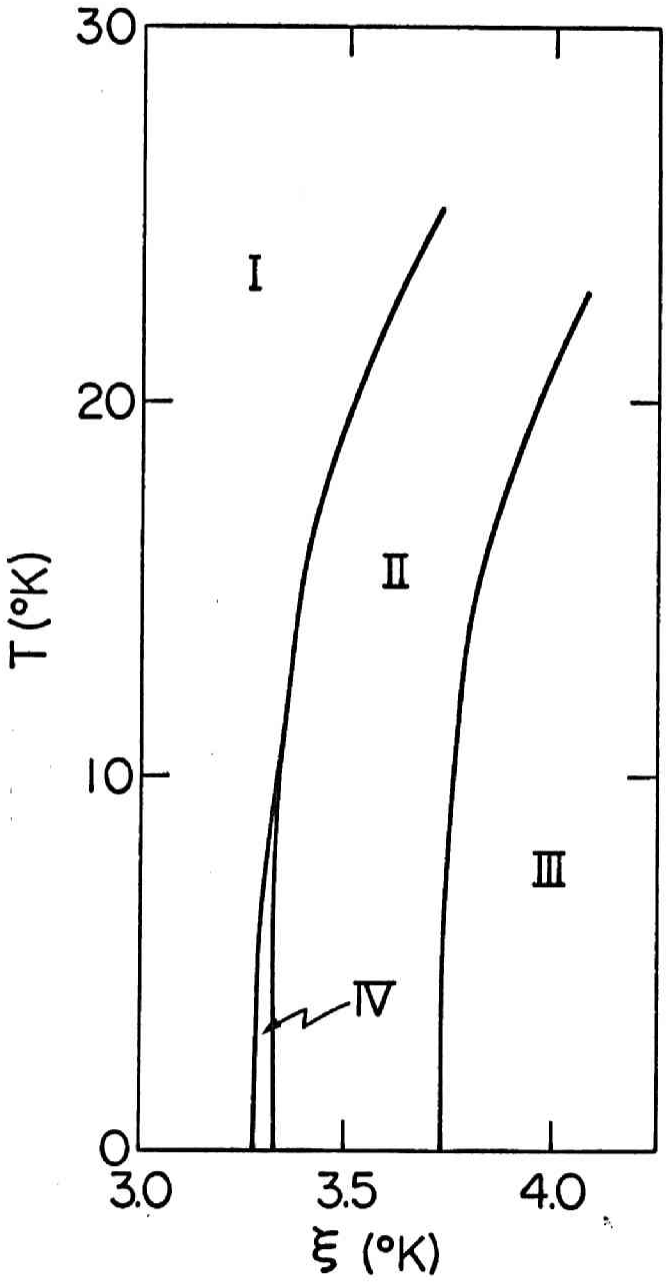

Fig. 7.

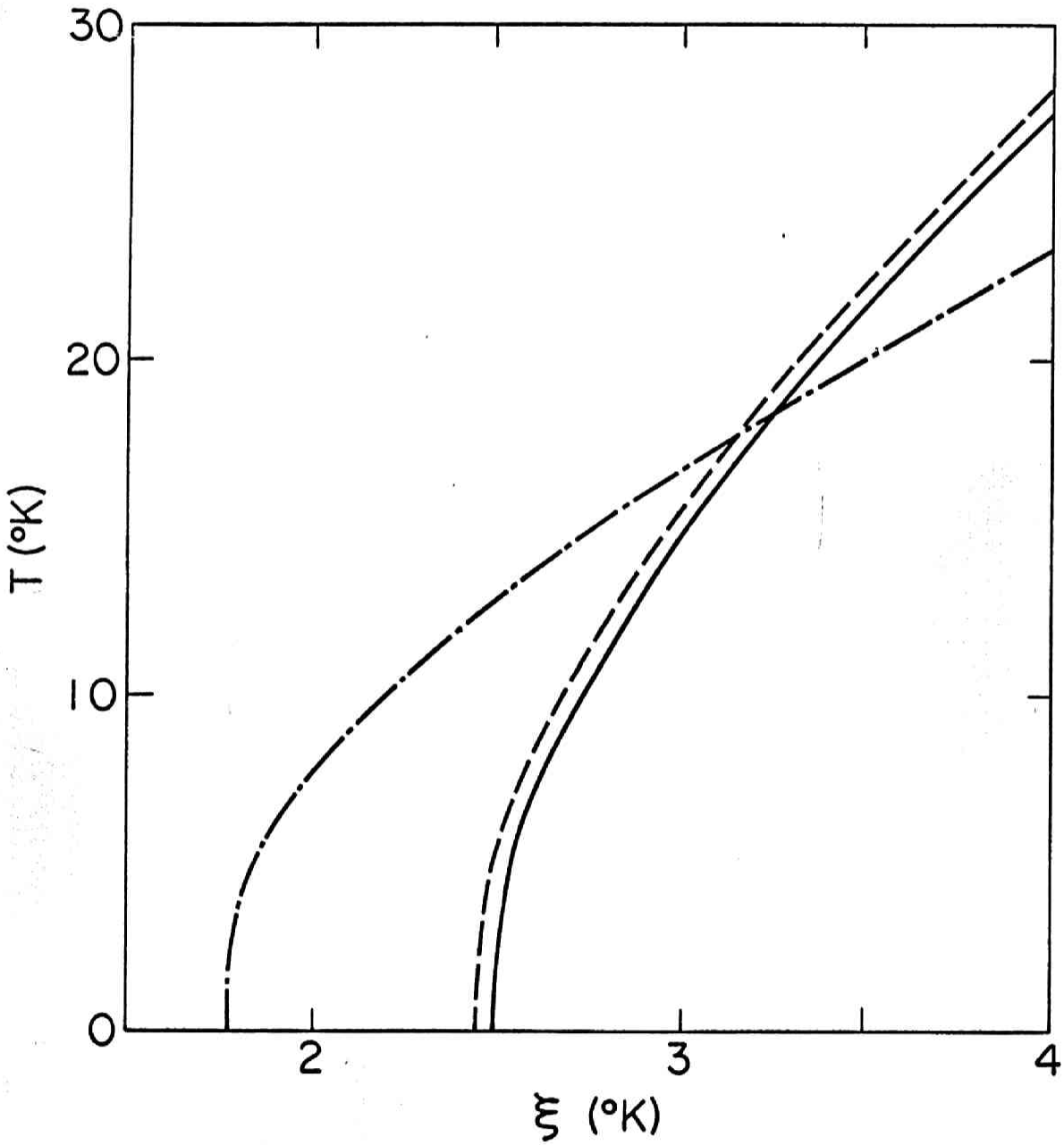

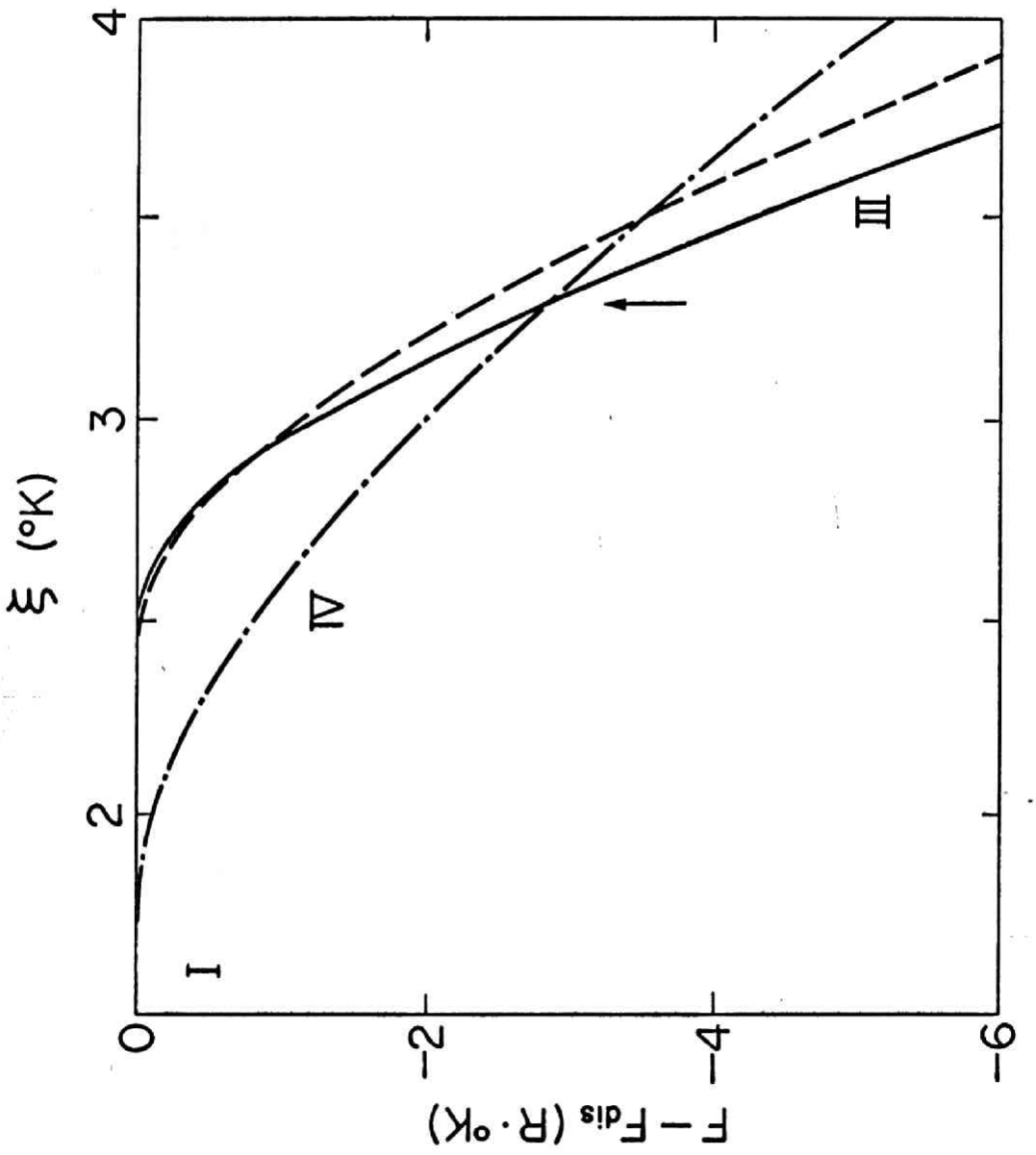

Fig. 8.

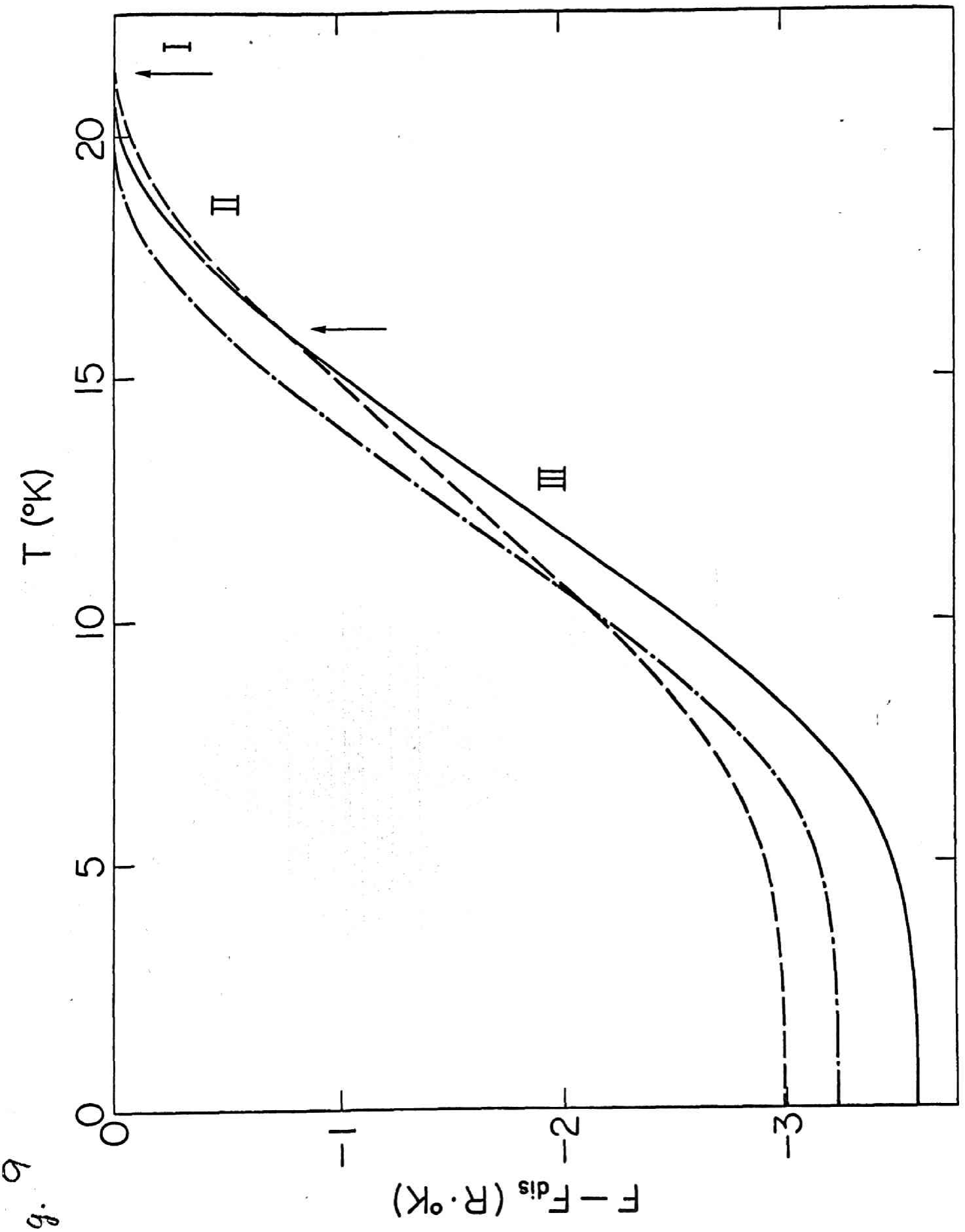

Fig. 9

Fig. 10.

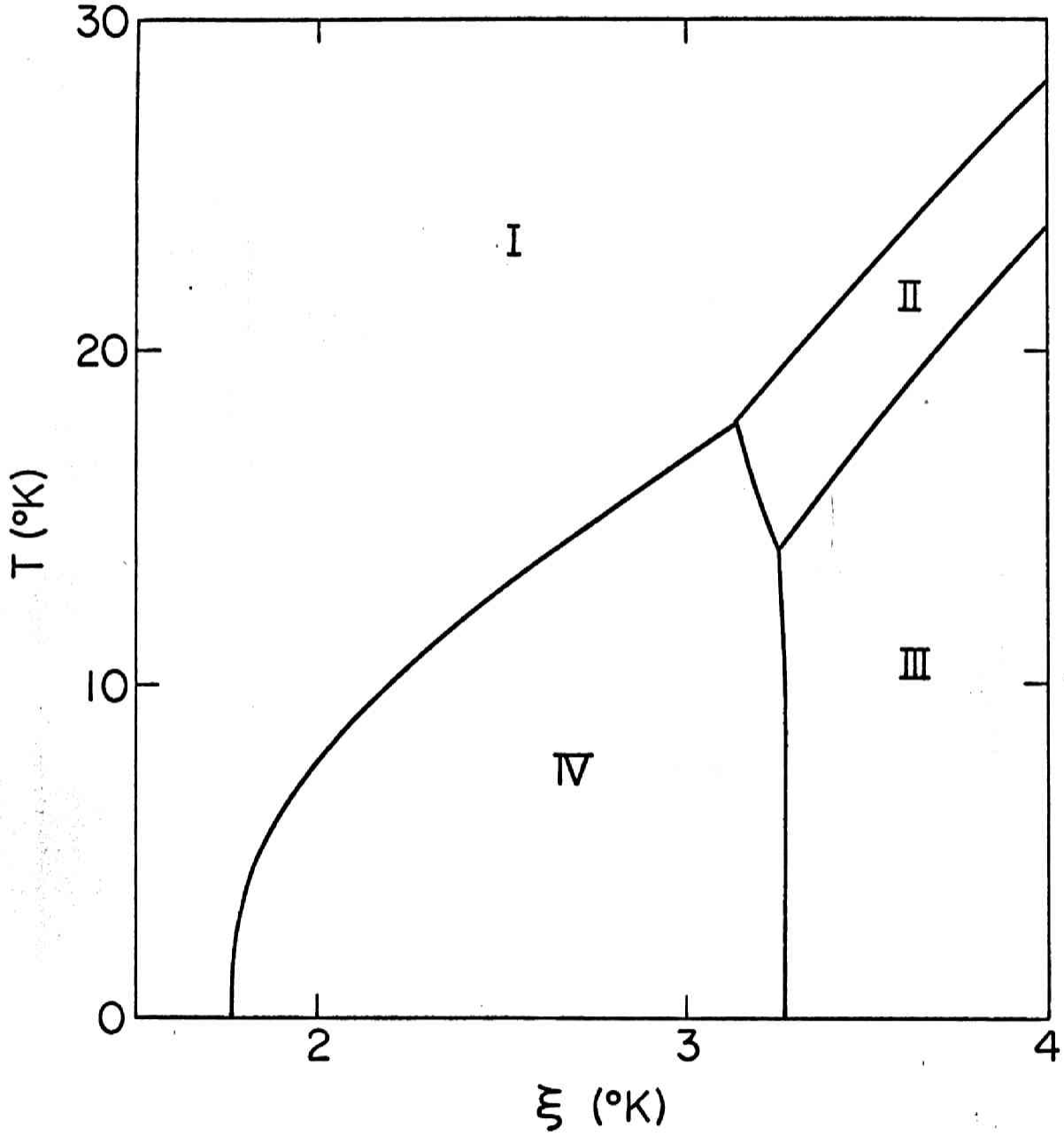

Fig. 11.

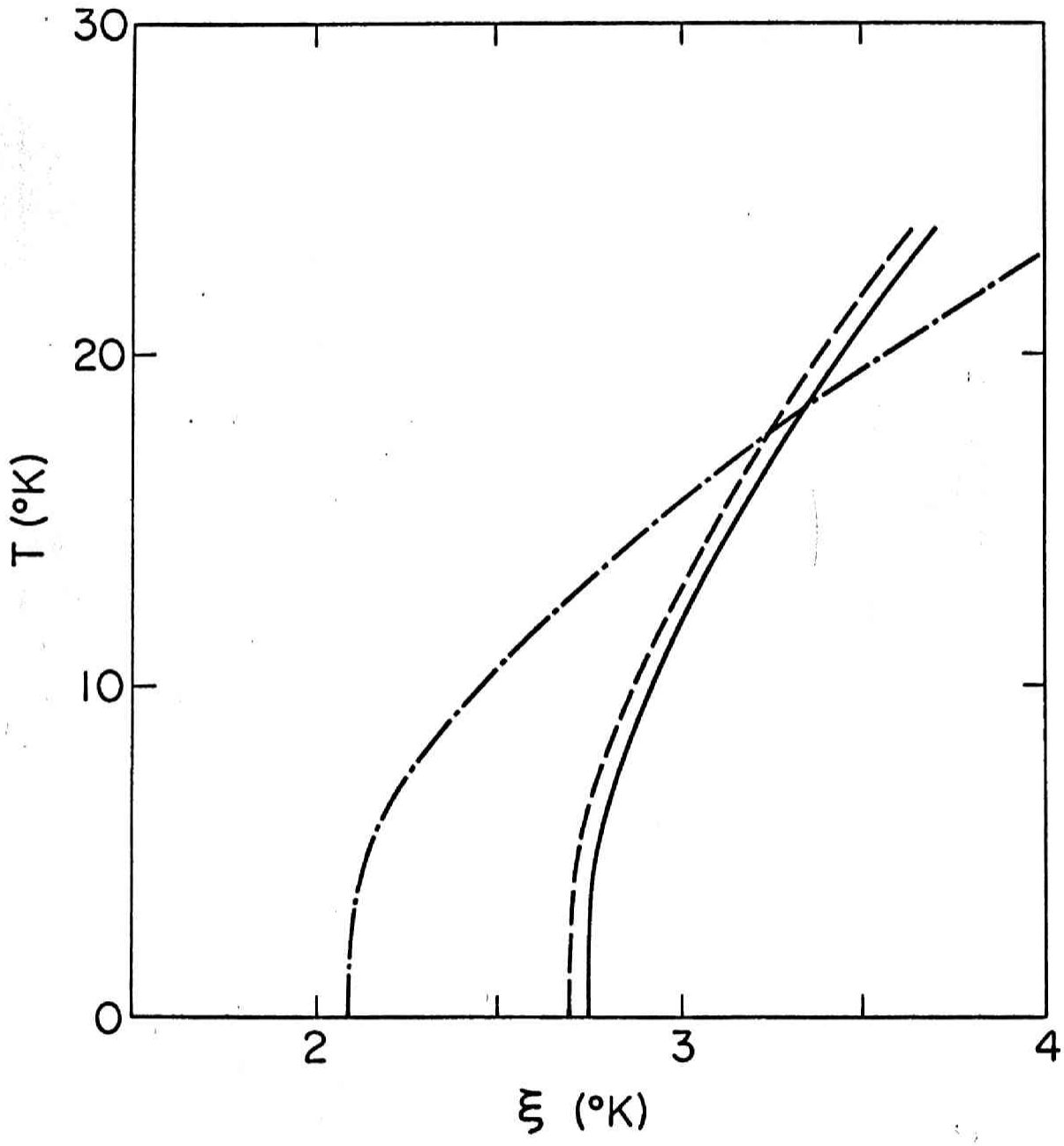

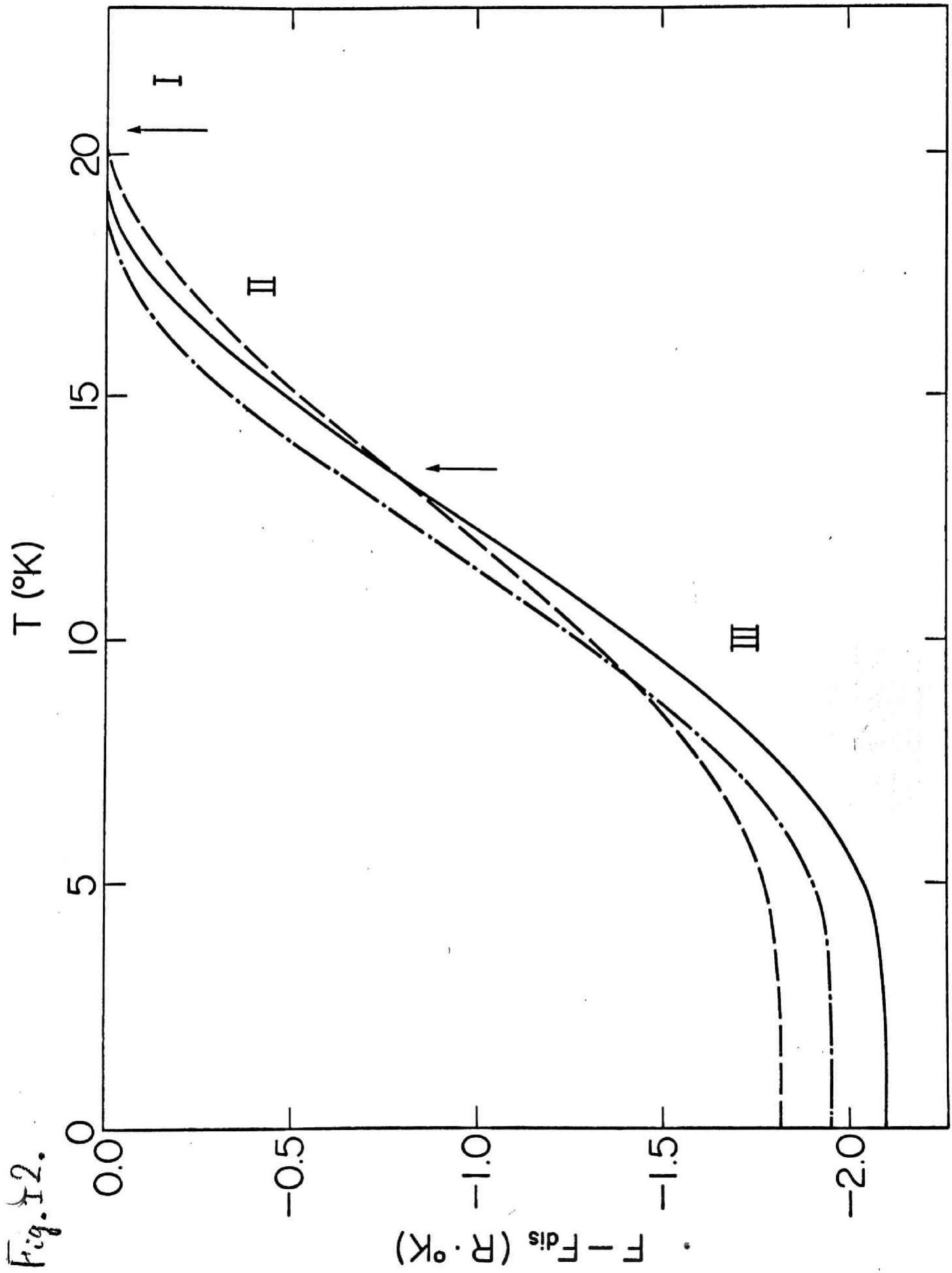

Fig. 12.

Fig. 13.

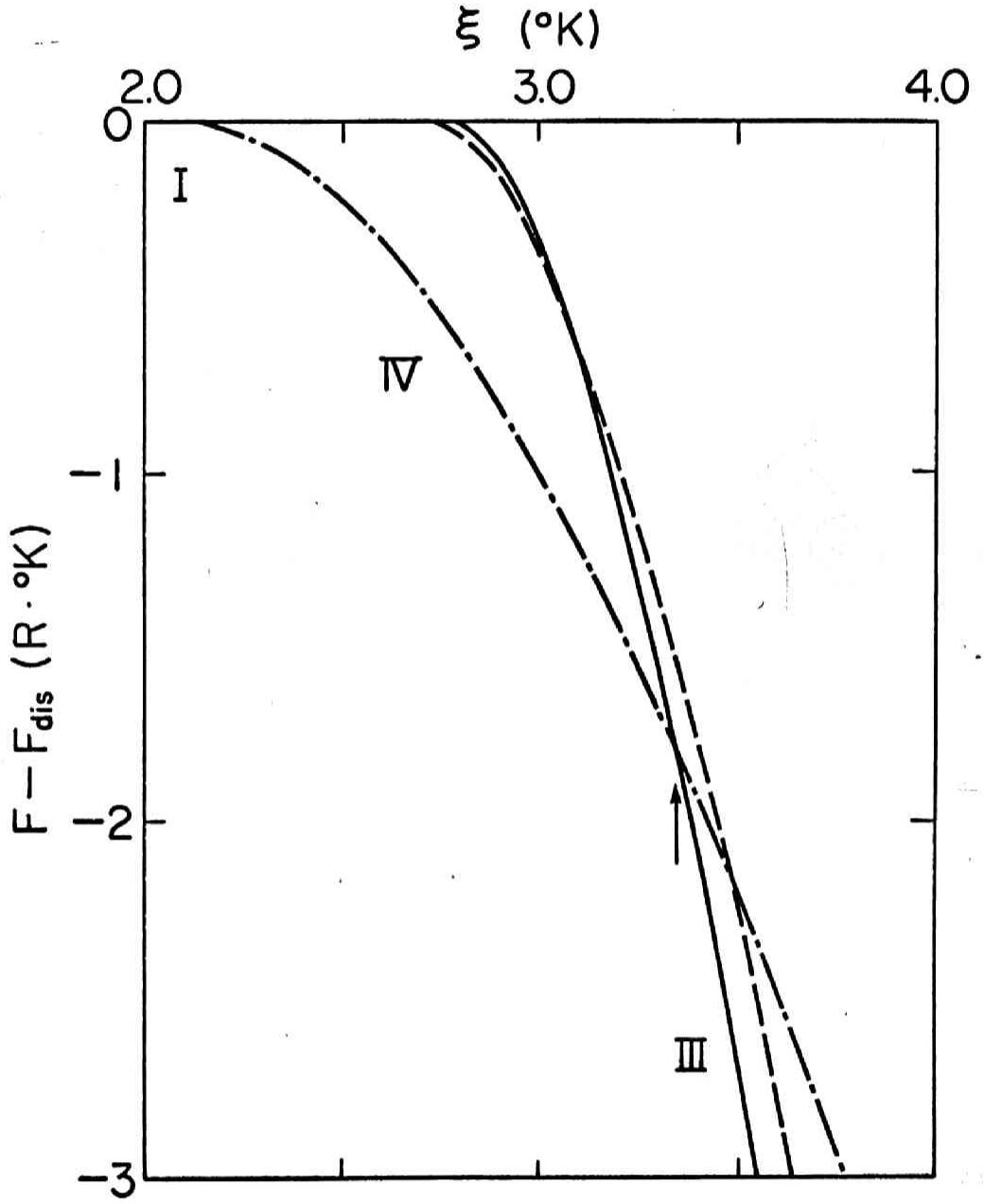

Fig. 14.

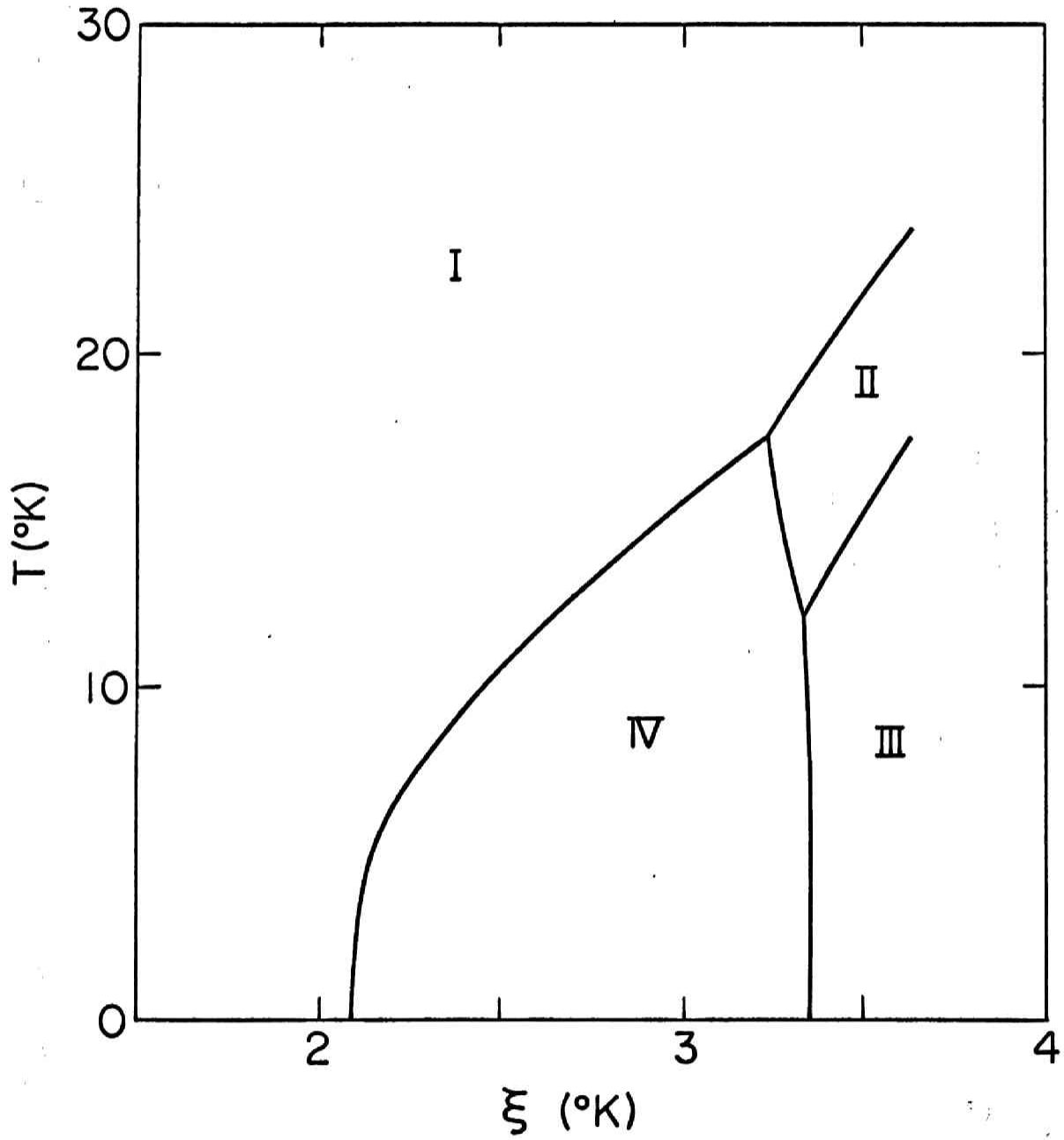

Fig. 15.

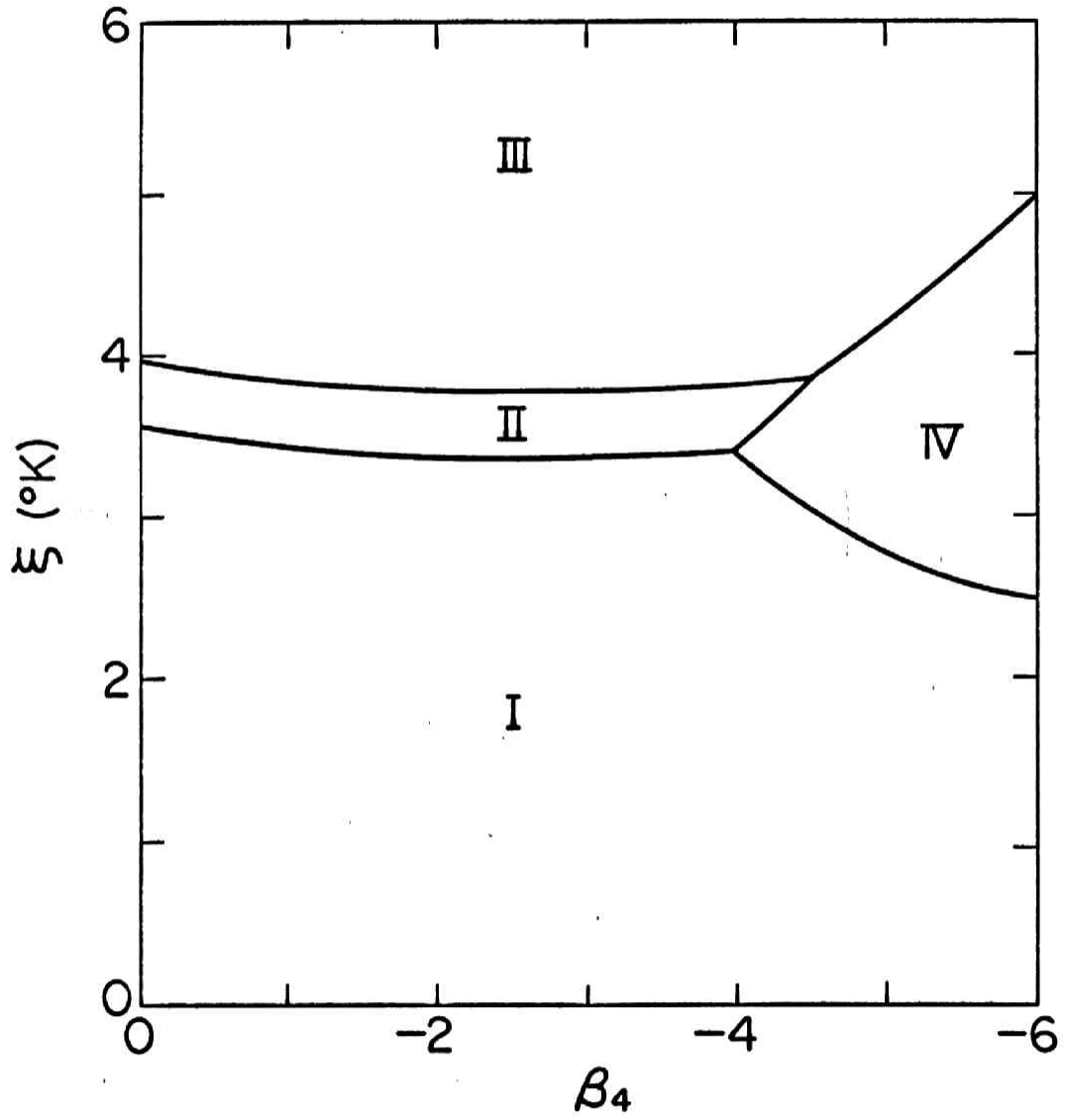

Fig. 16.